Electronic structure, magnetic properties, and magnetostructural transition in $Tb_5Si_{2.2}Ge_{1.8}$ from first principles

Durga Paudyal* and Y. Mudryk
The Ames Laboratory, US Department of Energy, Iowa State University, Ames, Iowa 50011-3020, USA

V. K. Pecharsky and K. A. Gschneidner Jr.
The Ames Laboratory, US Department of Energy, Ames, Iowa 50011-3020, USA and
Department of Materials Science and Engineering, Iowa State University, Ames, Iowa 50011-2030, USA
(Received 6 May 2011; revised manuscript received 7 June 2011; published 27 July 2011)

The electronic structure and magnetic properties of $Tb_5Si_{2.2}Ge_{1.8}$ have been studied from first principles electronic structure calculations. The total energy of the ferromagnetic (FM) orthorhombic [O(I)] $Tb_5Si_{2.2}Ge_{1.8}$ is lower than the total energy of the FM monoclinic (M) $Tb_5Si_{2.2}Ge_{1.8}$, indicating that the FM O(I) is the ground state structure of $Tb_5Si_{2.2}Ge_{1.8}$. Because of a strong 4*f*-5*d* exchange, the splitting of 5*d* bands of Tb atoms in the FM O(I) $Tb_5Si_{2.2}Ge_{1.8}$ is greater than that in the FM M $Tb_5Si_{2.2}Ge_{1.8}$, giving rise to higher 5*d* moments in the former. The magnetostructural transition temperature, T_M, and the isothermal magnetic entropy change, ΔS_M, have been calculated by coupling the parameters obtained from the first principles to the magnetothermodynamic models. Both T_M and ΔS_M are in good agreement with reported experimental values. The magnetic entropy change increases with decreasing magnetostructural transition temperature, which indicates a pathway toward tuning the magnitude of the magnetocaloric effect.

DOI: 10.1103/PhysRevB.84.014421 PACS number(s): 71.20.Eh, 71.15.Mb, 81.30.Kf

I. INTRODUCTION

Over the last decade, magnetic materials exhibiting giant magnetocaloric effect are at the forefront of research in materials physics because of their potential for applications in magnetic cooling.[1–4] The magnetic field–induced first-order phase transitions are responsible for the giant magnetocaloric effect.[5–10] To date, $Gd_5Si_xGe_{4-x}$ compounds are among the best prototypes showing a strong and reversible magnetocaloric effect in an alternating magnetic field when they undergo coupled magnetic and structural transitions. The concurrent change in the magnetization and crystal structure was observed in Gd_5Ge_4 and related materials through bulk magnetization and *in situ* x-ray powder diffraction studies.[10–13] Among the $Gd_5Si_xGe_{4-x}$ alloys, the largest magnetocaloric effect near room temperature is observed in $Gd_5Si_2Ge_2$ when the compound changes from the paramagnetic (PM) monoclinic (M) polymorph to the ferromagnetic (FM) orthorhombic [the so-called O(I)] polymorph. This change can be triggered by temperature,[12,14] magnetic field,[12,15] and/or hydrostatic pressure.[16,17] Thus, applied magnetic field above the Curie temperature transforms the compound from the PM M to the FM O(I) state,[18,19] during which the magnetic field dependence of the isothermal magnetization resembles that of a metamagnetic phase transition in an antiferromagnet.[20]

The $Tb_5Si_xGe_{4-x}$ compounds also exhibit the giant magnetocaloric effect in the intermediate range of compositions around $x = 2$.[21] Initially, it was believed that this system undergoes the coupled magnetostructural phase transformation identical to that found in $Gd_5Si_2Ge_2$.[22] However, unlike in $Gd_5Si_2Ge_2$, no clear metamagnetic-like behavior was observed in the magnetization of polycrystalline $Tb_5Si_2Ge_2$, and a follow up neutron powder diffraction study of this compound revealed a decoupling of the structural and magnetic transitions with a separation of ∼10 K.[23] This indicates that the monoclinic structure may also adopt a long-range ferromagnetic order in some members of the $R_5Si_xGe_{4-x}$ family, where R is a rare earth element, even though when R = Gd, long-range ferromagnetism is always associated with the O(I) polymorph.[24,25] Interestingly, the magnetic and structural transitions in $Tb_5Si_2Ge_2$ can be recoupled by a hydrostatic pressure of 8.6 kbar or higher, consequently enhancing the magnetocaloric effect of the compound by nearly 40% for a magnetic field change from 0 to 50 kOe.[26] A neutron diffraction study of a single crystal of $Tb_5Si_{2.2}Ge_{1.8}$, however, indicates that decoupling of the magnetic and crystallographic transitions, if any, must be smaller than ∼5 K,[27] thus pointing toward a compositional (x) dependence of the degree of decoupling. Because no intermediate magnetic-only transition of the monoclinic phase was detected within 5 K of the crystallographic transition in $Tb_5Si_{2.2}Ge_{1.8}$, it appears that the extent of the decoupling is decreasing with increasing concentration of Si. The recent measurements of $Tb_5Si_{2.2}Ge_{1.8}$[28] indicate that the decoupling is within the 5 K range.

First principles calculations performed on $Gd_5Si_2Ge_2$,[29–36] Gd_5Ge_4,[37–41] $Gd_5Si_{0.5}Ge_{3.5}$,[42] $Gd_5Sb_{0.5}Ge_{3.5}$,[43] Ho_5Ge_4,[44] $Ho_5Si_{3.2}Ge_{0.8}$,[45] and Ho_5Si_4[46] indicate that chemical bonding and crystallography play a major role in defining the magnetic properties of these compounds. The breaking and reforming of the interslab T-T dimers,[14] which accompanies the O(I)-M and O(I)-O(II) structural transitions [the O(II) phase is an orthorhombic polymorph that is different from O(I), see Refs. 5, 9 for details), and the related nearly 1 Å elongation and contraction, respectively, of the interslab T-T bonds affect both the location of the Fermi level and the effective magnetic exchange coupling, J_0.[29,32] Comparing the FM ordered O(I) phase of $Gd_5Si_2Ge_2$ with the hypothetical FM M $Gd_5Si_2Ge_2$, the former is characterized by larger 5*d* magnetic moments of the Gd atoms and a larger J_0 than those of the latter, thus explaining the stability of the O(I) structure in the ferromagnetically ordered state. The different

polymorphs (i.e. the monoclinic (M) and orthorhombic O(I) phases in $Gd_5Si_2Ge_2$), have different T_Cs and, therefore, different temperature dependencies of the magnetization.[29]

When PM M $Gd_5Si_2Ge_2$ is cooled, its free energy remains lower than that of the FM O(I) $Gd_5Si_2Ge_2$ below the Curie temperature of the latter. The actual temperature of the magnetostructural transition of $Gd_5Si_2Ge_2$, T_M, is located between ${T_C}^M$ and ${T_C}^{O(I)}$. Hence, when the free energies of the two polymorphs become equal at T_M, the O(I) $Gd_5Si_2Ge_2$ phase is already well below its ${T_C}^{O(I)}$. As a result, the polymorphic transition at T_M also involves the ferromagnetic ordering with a large, discontinuous increase of spontaneous magnetization. When a magnetic field is applied just above T_M, it changes the balance of the free energies between the PM M and FM O(I) $Gd_5Si_2Ge_2$ phases, which in turn triggers a crystallographic transition between the two polymorphs that have different magnetizations, leading to a metamagnetic-like, discontinuous change of the magnetization at various temperature-specific critical fields.

Given that $Tb_5Si_{2.2}Ge_{1.8}$ has the same sequence of polymorphs with the same type of crystal structures as $Gd_5Si_2Ge_2$, the metamagnetic-like transitions in $Tb_5Si_{2.2}Ge_{1.8}$ are expected to have a similar mechanism, but the single-ion anisotropy of the Tb^{3+} ion and the orbital angular momentum quantum number L = 3 are considerable, giving rise to spin orbit and crystalline electric field interactions in $Tb_5Si_{2.2}Ge_{1.8}$ when compared with the negligible single-ion anisotropy and L = 0 of the Gd^{3+} ion in $Gd_5Si_2Ge_2$. Therefore, the first goal of this work is to evaluate the total energies and magnetic moments, including orbital moments of the O(I) and M structures of $Tb_5Si_{2.2}Ge_{1.8}$, compute magnetic exchange interactions considering the Heisenberg approach for the nearest neighbor slabs, and then calculate the Curie temperatures utilizing the mean field relation. The next goal is to analyze finite temperature properties, such as the magnetic free energy and magnetic entropy by coupling first principles outputs such as saturated magnetic moments, including orbital moments and Curie temperatures, to the magnetothermodynamic models in order to calculate the magnetostructural transition temperature and magnetic entropy change.

II. CRYSTAL AND MAGNETIC STRUCTURES OF $Tb_5Si_{2.2}Ge_{1.8}$

From neutron diffraction[27] and x-ray diffraction[47] studies, it has been established that the ground state structure of $Tb_5Si_{2.2}Ge_{1.8}$ is orthorhombic (space group Pnma), Gd_5Si_4 type, also known as O(I).[48] Above ~107 K, it transforms into the monoclinic (space group $P112_1/a$) $Gd_5Si_2Ge_2$-type crystal structure, also known as M.[48] The $Gd_5Si_2Ge_2$-type polymorph is a martensitic-like distortion of the Gd_5Si_4-type orthorhombic structure. These structures are shown in Fig. 1.

The two polymorphs of $Tb_5Si_{2.2}Ge_{1.8}$ may be conveniently described in terms of nearly two-dimensional, ~7 Å thick slabs formed by strongly bonded Tb, Si, and Ge atoms.[5,14,21,26] Here, T1 in the O(I) and T1a, T1b in the M structures represent Si and Ge atoms statistically (0.40 Si + 0.60 Ge) mixed in the interslab positions, henceforth referred as the T′ sites, whereas T2 and T3 (0.67 Si + 0.33 Ge) in both structures represent the Si and Ge atoms in the intraslab positions

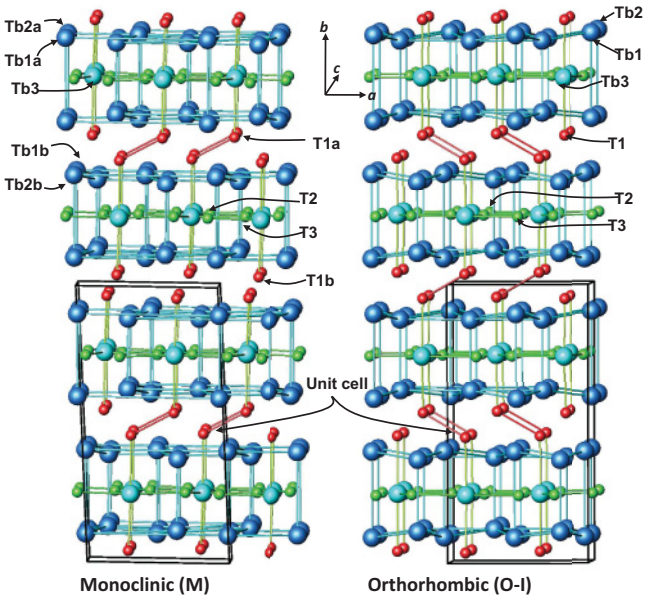

FIG. 1. (Color online) The crystal structures of the monoclinic (left) and orthorhombic (right) phases of $Tb_5Si_{2.2}Ge_{1.8}$. T1 in the orthorhombic and T1a, T1b in the monoclinic structures represent the Si/Ge atoms in the interslab positions (T′ sites), and T2, T3 in both phases represent the Si/Ge atoms in intraslab positions (T sites).

(henceforth the T sites). The -Tb-T′-T′-Tb- interslab networks are continuous in the low-temperature O(I) polymorph. But at high temperatures (in the M polymorph), these networks are no longer continuous because of a substantial elongation (bond distances are increasing from 2.81 to 3.45 Å)[47] of every other T′-T′ bond distance. When temperature is reduced, the process is reversible (i.e., the slabs reverse the movements with respect to one another in a shear fashion and the interslab networks become continuous).

The ground state O(I) structure of $Tb_5Si_{2.2}Ge_{1.8}$ is ferromagnetic. Interestingly, above ~107 K, it transforms to the monoclinic polymorph but remains ferromagnetic up to ~112 K, indicating a weakly decoupled magnetostructural transition in this compound.[28] Above ~112 K, FM M $Tb_5Si_{2.2}Ge_{1.8}$ transforms to the PM state via a conventional second-order phase transition.

III. THEORETICAL APPROACH

The local spin density approximation including Hubbard U parameter (LSDA + U) approach[49,50] has been employed to investigate the electronic structure and magnetic properties of the $Tb_5Si_{2.2}Ge_{1.8}$ system. Using LSDA + U, the localized 4*f* electrons of Tb atoms in this system can be suitably treated. The LSDA + U method starts from the LSDA total energy, which is supplemented by an additional intra-atomic Coulomb correlation term *U* and exchange interaction term *J* of multiband Hubbard type, minus a so-called double counting term to subtract the electron-electron interactions already included in LSDA. Our calculations have been performed using the scalar relativistic version (which includes the mass velocity and Darwin correction terms) of the LSDA + U method implemented in the tight-binding linear muffin tin orbital (TB-LMTO).[51] Because the difference between the

occupied energy levels (determined from photoemission spectroscopy) and the unoccupied energy levels (determined from bremsstrahlung isochromatic spectroscopy) of Tb[52] and Gd[49] are nearly identical after neglecting spin orbit coupling, we employed $U = 6.7$ eV and $J = 0.7$ eV—the well-known values for Gd atoms—also for Tb atoms in $Tb_5Si_{2.2}Ge_{1.8}$. In these calculations, the conventional von Barth and Hedin parameterization of the LSDA[53] has been adopted, which is one of the well-known local exchange correlation functionals. Furthermore, we have used 125 and 170 special k points in the irreducible part of the Brillouin zone for k-space integration in the orthorhombic and monoclinic phases, respectively.

To check the effect of full potential in these O(I) and M structures of $Tb_5Si_{2.2}Ge_{1.8}$, we have also employed the full potential linear augmented plane wave (FP-LAPW) method for the electronic structure calculations. This method yields results similar to TB-LMTO, indicating that the TB-LMTO method with atomic sphere approximation (which is much faster than the FP-LAPW) is also suitable for electronic structure calculations of $Tb_5Si_{2.2}Ge_{1.8}$. Therefore, here, we show only the electronic structure results obtained from the TB-LMTO method and couple these results to the magnetothermodynamic models for estimation of finite temperature properties.

As stated in the previous section, diffraction experiments[47] indicate a mixed occupancy of Si and Ge atoms in the T′ and T sites of $Tb_5Si_{2.2}Ge_{1.8}$. The 60% Ge and 40% Si occupy the T′ positions, whereas 33% Ge and 67% Si occupy the T positions in both the O(I) and M structures of $Tb_5Si_{2.2}Ge_{1.8}$. For theoretical calculations, two different mixing approaches were employed to incorporate both Si and Ge in the appropriate sites. The Ge atoms were placed in all T′ and T sites as a first model and then Si atoms in all T′ and T positions as a second model in the first approach. The 45% of outputs from the first model and 55% outputs from the second model constitute the final outputs. In the second approach, we locate Ge atoms in the T′ and Si atoms in the T positions as a third model and then Si in the T′ and Ge in the T positions as a fourth model. Then, we take weighted averages of the outputs from the third and fourth models according to the experimentally determined occupancies of the interslab and intraslab sites by Ge and Si atoms.

The magnetic interactions in $Tb_5Si_{2.2}Ge_{1.8}$ are mainly due to indirect (i.e., Ruderman–Kittel–Kasuya–Yosida [RKKY][54]) Tb 4*f*–Tb 4*f* exchange mediated by the spin-polarized 5*d* electrons. The origin of this 4*f*-4*f* exchange is the 4*f*-5*d* exchange, and, therefore, the changes in the 4*f*-5*d* exchange reflect the changes in the 4*f*-4*f* interactions when one structure is replaced by another. Hence, we estimate the 4*f*-5*d* exchange interactions of Tb atoms in the O(I) and M structures of $Tb_5Si_{2.2}Ge_{1.8}$. Recently, this approach has been successfully applied to the Gd_5Ge_4 system,[38] and for theoretical details and application to other rare earth–based materials, we refer interested readers to Refs. 55–58.

The interactions between orbital states of magnetic ions and crystalline electric fields are typical for rare earth materials. The crystal field has site-matching symmetry, which gives rise to a strong coupling between the 4*f* orbital moment and the crystal lattice. This coupling may be transferred to the spin moments via spin orbit coupling. As a result, an interesting interplay between spin orbit interactions, crystalline electric field, and exchange interactions often occurs in lanthanide containing intermetallic compounds. In Gd-based materials, Gd^{3+} ions have negligible single-ion anisotropy; therefore, the indirect 4*f*-4*f* exchange, mediated by spin-polarized conduction electrons, dominates over the crystalline electric field–coupled spin orbit mechanism. A study of multiplet effects in the electronic structure of heavy rare earth metals[52] indicates that the spin orbit constant in Tb metal is 0.24 eV/Tb, which is identical to the value of a single Tb ion.[59] This may imply that in the metallic Tb, the crystalline electric field effect, which also depends on the orbital moment, has the same value as that of a single Tb^{3+} ion (e.g., Steven's second-order parameter for Tb^{3+} ion is $-1/99$[60]). The FP-LAPW calculations with the inclusion of spin orbit coupling show the same orbital moments (3.02 μ_B /Tb orbital moment [3 μ_B contributed from 4*f* and 0.02 μ_B from 5*d* electrons]) for both the O(I) and M polymorphs of $Tb_5Si_{2.2}Ge_{1.8}$. The orbital moment contributions from 4*f* Tb and 5*d* Tb electrons have not been determined from experimental data, although it may be possible to do so from recent x-ray magnetic circular dichroism measurements on the magnetostructural properties of $Tb_5(Si_xGe_{1-x})_4$.[61] Because the M structure is a distorted O(I) structure, identical orbital moments in both the O(I) and M structures are not surprising. The results shown below include orbital moments together with the spin moments of Tb atoms in both structures of $Tb_5Si_{2.2}Ge_{1.8}$.

IV. RESULTS AND DISCUSSION

Experimental observations[47] show that $Tb_5Si_{2.2}Ge_{1.8}$ transforms from the FM O(I) phase to the FM M variant at ∼107 K, but FM M transforms to PM M at ∼112 K, indicating a narrowly decoupled magnetostructural transition. To theoretically determine the ground state structure of $Tb_5Si_{2.2}Ge_{1.8}$, the total energies were calculated in both the O(I) and M structures. The total energy of the FM O(I) is lower than that of the FM M by 3.66 eV/cell from the first mixing approach and 3.63 eV/cell from the second mixing approach (both approaches were discussed in the previous section), which confirms that the FM O(I) is indeed the ground state structure of $Tb_5Si_{2.2}Ge_{1.8}$.

To probe the relative stabilities of the O(I) and M phases of $Tb_5Si_{2.2}Ge_{1.8}$, the phase formation energies (E_f) have been calculated from the total energies of the alloy and the components using the following relation:

$$E_f = E_{Tb_5Si_{2.2}Ge_{1.8}} - c_{Tb}E_{Tb} - c_{Si}E_{Si} - c_{Ge}E_{Ge}.$$

Here, E and c denote total energy and molar fractions, respectively. The difference in the formation energies of the two phases is the energy required to transform one phase into the other. The computed formation energies of both the O(I) and M phases are negative. The E_f of the FM O(I) $Tb_5Si_{2.2}Ge_{1.8}$ is lower compared with the FM M $Tb_5Si_{2.2}Ge_{1.8}$. But E_f for the PM M $Tb_5Si_{2.2}Ge_{1.8}$ is lower than that of the FM M for $Tb_5Si_{2.2}Ge_{1.8}$ (Table I). These results indicate that the O(I) $Tb_5Si_{2.2}Ge_{1.8}$ is stable in the FM ordered state and that the M $Tb_5Si_{2.2}Ge_{1.8}$ is stable in the magnetically disordered state. Interestingly, the formation energy of the FM O(I) phase of $Tb_5Si_{2.2}Ge_{1.8}$ is higher by 39% than the same of the FM O(I) phase of $Gd_5Si_2Ge_2$,[29] which indicates greater thermodynamic stability of the FM O(I) $Gd_5Si_2Ge_2$ compared

TABLE I. Phase formation energies calculated using two different mixing approaches. In the first mixing approach, the Ge atoms were placed in all T′ and T sites as a first model and then Si atoms in all T′ and T positions as a second model. The 45% of outputs from the first model and 55% from the second model constitute the final output. In the second mixing approach, we locate Ge atoms in the T′ and Si in the T positions as a third model and then Si in the T′ and Ge in the T positions as a fourth model. Weighted averages of the outputs from the third and fourth models are calculated according to the experimentally determined occupancies of the interslab and intraslab sites by Ge and Si atoms.

	Phase formation energy (meV/atom)	
Phase	First mixing approach	Second mixing approach
O(I) FM	−819.9	−822.7
O(I) PM	−714.8	−717.9
M FM	−717.3	−721.8
M PM	−724.0	−727.9

with the FM O(I) $Tb_5Si_{2.2}Ge_{1.8}$. This difference is consistent with a gradual reduction of the degree of transformation of the M phases into the O(I) phases observed on cooling in the series $Gd_5Si_2Ge_2$[62] → $Tb_5Si_{2.2}Ge_{1.8}$[47] → Dy_5Si_3Ge[63] → $Ho_5Si_{3.2}Ge_{0.8}$[45] → Er_5Si_4,[64] which is respectively lowered from ∼95% to ∼80%, ∼50%, 0%, and 0%.

Table II shows that the 5*d* exchange splitting in the FM O(I) $Tb_5Si_{2.2}Ge_{1.8}$ is higher than the same in the FM M $Tb_5Si_{2.2}Ge_{1.8}$, giving rise to higher 5*d* moments in the O(I) polymorph. The magnetic moments of Tb atoms in both structures are shown in Table III. Because of the anisotropy in the nearest neighbor distances, the 5*d* magnetic moments of the nonequivalent sites of Tb atoms are variable in both the O(I) and M structures. The magnetic moments of Tb3 atoms (which are located in the middle of the slabs and play a key role in forming the -Tb-T′-T′-Tb- networks that are continuous in the O(I) and discontinuous in the M $Tb_5Si_{2.2}Ge_{1.8}$) are larger compared with other nonequivalent Tb atoms (which are located on the surfaces of the slabs) in both FM O(I) and FM M $Tb_5Si_{2.2}Ge_{1.8}$. Hence, the Tb3 atoms occupying 4*c* sites in both the O(I) and M polymorphs may have a strong influence on the overall magnetism of the compound.

To probe how the structural change affects the electronic structure and magnetism of $Tb_5Si_{2.2}Ge_{1.8}$, the 5*d*-Tb and 4*p*-Ge densities of states (DOS) were calculated, with the FM order imposed in both the O(I) and M structures. Figure 2 shows that the average 5*d* DOS at the Fermi level in the FM O(I) is higher compared with FM M $Tb_5Si_{2.2}Ge_{1.8}$. The degree of spin polarization, $\eta = \frac{D^{\uparrow}(E_F)-D^{\downarrow}(E_F)}{D^{\uparrow}(E_F)+D^{\downarrow}(E_F)}$ is also higher by 43% in the O(I) structure. The integrated number of 5*d* electrons up to the Fermi level and spin-up and -down band splitting are also higher by 23% and 8%, respectively, in the O(I) $Tb_5Si_{2.2}Ge_{1.8}$. Therefore, spin polarization plays a main role in the stability of the O(I) phase in the FM state compared with the M polymorph, in agreement with the total energy analysis.

TABLE II. The average 5*d* spin splitting of Tb atoms in the FM O(I) and FM M structures of $Tb_5Si_{2.2}Ge_{1.8}$.

	5*d* Splitting energy (meV/Tb)	
Population of T and T′ sites	FM O(I)	FM M
Ge in both T′ and T sites	511	474
Si in both T′ and T sites	506	469
Ge in T′ and Si in T sites	505	462
Si in T′ and Ge in T sites	509	480

Figure 3 shows total DOS at E_F assuming different occupations of the interslab T′ and intraslab T positions. The DOS (E_F) is always higher in the FM O(I) than in the FM M, regardless of the differences in occupations of the interslab and intraslab T′ and T positions. Because the spin-down DOS (E_F) is similar in all cases, the differences are only shown for the spin-up DOS (E_F), which therefore indicates the differences in the spin polarization with different possibilities of occupation of T and T′ sites. Placing Si atoms in the inter- and intraslab positions instead of Ge atoms enhances the number of electrons at the Fermi level, except for the case with the interslab Ge and intraslab Si in the O(I) $Tb_5Si_{2.2}Ge_{1.8}$ phase, in which the density of states falls in a valley of the majority bands instead of a peak. This is peculiar for $Tb_5Si_{2.2}Ge_{1.8}$ because in $Gd_5Si_{0.5}Ge_{3.5}$,[42] the DOS (E_F) is higher with intraslab Si substitution. Nevertheless the variability of the DOS (E_F) assuming different occupations of Ge and Si in both O(I) and M polymorphs are reflected in the magnetic exchange interactions and the Curie temperatures shown in Table IV.

Figure 4 compares the average DOS of all Tb atoms and DOS for Tb3 atoms (located in the middle of the slabs). Both behave similarly, but the DOS averaged over all Tb atoms is lower than that of the Tb3 atom at the Fermi level in either polymorph. Also the DOS (E_F) of the Tb3 atom is higher in the O(I) than the same in the M polymorph. These results, therefore, provide further evidence that the Tb3 atoms play a key role in the magnetism of $Tb_5Si_{2.2}Ge_{1.8}$.

Because Tb3 atoms from one slab are connected to Tb3 from the neighboring slabs, either through the short T′-T′ pairs in the O(I) structure or through alternatively short and long T′-T′ pairs in the M structure, the difference in the overlap between the 5*d* states of Tb and the 4*p*/3*p* states of T′ should be responsible for the difference in the interslab coupling in these two structure types. To examine these overlaps, for example, the average 5*d* DOS of all Tb atoms and average 4*p* DOS of interslab Ge atoms in both structures are compared in Fig. 5. The spin-up 4*p* DOS of Ge at E_F is slightly higher than the spin-down 4*p* DOS of Ge in the O(I) structure, which indicates a small 4*p* spin polarization induced by 5*d* electrons of Tb in this polymorph. On the other hand, the spin-up and spin-down 4*p* DOS (E_F) are identical in the M polymorph, indicating no 4*p* spin polarization in the M polymorph. The 3*p* DOS of Si behaves similarly but shows slightly higher spin polarization at the Fermi level compared with that of 4*p* Ge. There is 70% 5*d*-Tb and 30% 4*p*-Ge hybridization at about −0.5 eV in the spin-down bands of the M polymorph, but both spin-down 5*d*-Tb and 4*p*-Ge are zero at this energy range in the O(I) structure. These results, therefore, indicate that when the O(I) polymorph transforms to the M polymorph, the spin-down 4*p*/3*p* states that are pushed toward the Fermi level because of the weak T′-T′ bonding hybridize with 5*d*

TABLE III. Magnetic moments of Tb atoms in the FM O(I) and FM M polymorphs of $Tb_5Si_{2.2}Ge_{1.8}$.

	Magnetic moment (μ_B)				
Atom	Ge in T′ and T sites	Si in T′ and T sites	Ge in T′ and Si in T sites	Si in T′ and Ge in T sites	Expt. 27
FM O(I)					
Tb1	9.31	9.32	9.31	9.33	9.30
Tb2	9.29	9.27	9.27	9.27	9.20
Tb3	9.44	9.43	9.42	9.44	9.60
FM M					
Tb1a	9.24	9.25	9.22	9.26	
Tb1b	9.19	9.18	9.16	9.20	
Tb2a	9.25	9.24	9.22	9.27	
Tb2b	9.19	9.18	9.17	9.20	
Tb3	9.33	9.32	9.31	9.35	

states and reduce the magnetic moments of Tb atoms in the M polymorph.

The influence of 4*f* spins on 5*d* electrons has been further examined through the calculations of the 4*f*-5*d* exchange interactions in both structures. On average, the 4*f*-5*d* exchange interactions in the O(I) $Tb_5Si_{2.2}Ge_{1.8}$ are stronger by 10% when compared with that in the M $Tb_5Si_{2.2}Ge_{1.8}$. This is smaller than the 20% difference in the 4*f*-5*d* exchange interactions between the O(I) and M structures of $Gd_5Si_2Ge_2$. In $Gd_5Si_2Ge_2$, there is a coupled magnetostructural transition and a 30% increase in the lengths of interslab T′-T′ bonds during a transformation from the low-temperature FM O(I) structure to the high-temperature PM M polymorph. A similar 30% increase in the interslab T′-T′ bond lengths, but a smaller change in the 4*f*-5*d* exchange interactions in $Tb_5Si_{2.2}Ge_{1.8}$ compared with $Gd_5Si_2Ge_2$, can be related to the competition between magnetic energy and strain energy (the change in the unit cell dimensions in $Tb_5Si_{2.2}Ge_{1.8}$ is highly anisotropic, and the difference in phase volumes exceeds 0.7%[47]). The calculations show that the strain energy associated with the O(I) to M transformation is higher by ∼7% in $Tb_5Si_{2.2}Ge_{1.8}$ than in $Gd_5Si_2Ge_2$. Here, the strain energy is estimated by calculating the nonmagnetic total energy difference between the O(I) and M polymorphs. The increase in strain energy is not immediately compensated by the magnetic exchange energy, and $Tb_5Si_{2.2}Ge_{1.8}$ remains in the ferromagnetic state in the M $Tb_5Si_{2.2}Ge_{1.8}$ polymorph over a small range of temperatures. This conclusion is also consistent with the lower percentage (80%) of completion of the M to O(I) transformation in $Tb_5Si_{2.2}Ge_{1.8}$ compared with $Gd_5Si_2Ge_2$ (95%), as mentioned above, and also because the formation energy of FM O(I) in the $Tb_5Si_{2.2}Ge_{1.8}$ is 39% higher than in FM O(I) $Gd_5Si_2Ge_2$.

Because the 4*f* magnetic moments of Tb are localized, the Heisenberg-type Hamiltonian for the dependence of energy on spin configuration may be applied to $Tb_5Si_{2.2}Ge_{1.8}$ assuming indirect RKKY-type exchange interactions. The spin Hamiltonian with zero external magnetic fields is given by[65]

$$H = -\sum_i \sum_\delta j_{i,i+\delta} \vec{S}_i \vec{S}_{i+\delta},$$

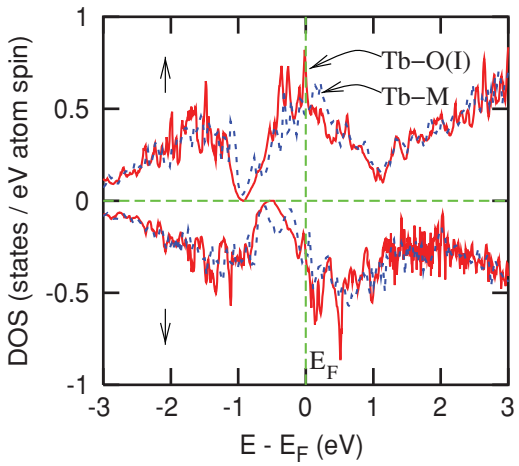

FIG. 2. (Color online) Comparison of the average 5*d* density of states (DOS) of all Tb atoms in the O(I) and the M structures of $Tb_5Si_{2.2}Ge_{1.8}$. The DOS at E_F and the exchange splitting of 5*d* bands are higher in the O(I) structure. Here and in all other DOS figures, the vertical arrows indicate the majority (spin-up) and minority (spin-down) bands, respectively.

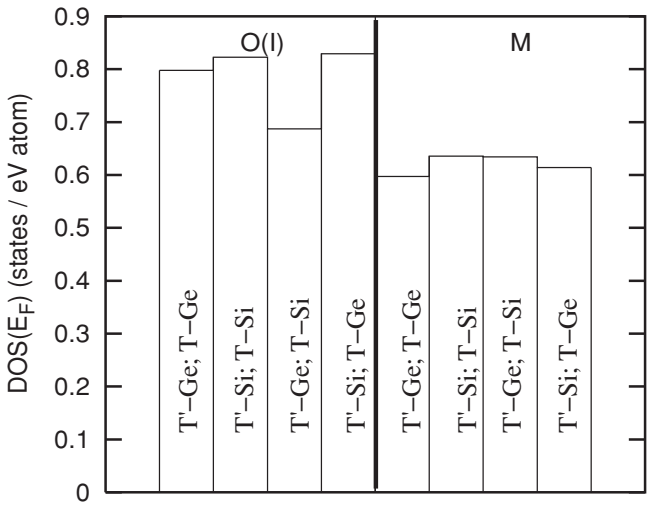

FIG. 3. Comparison of density of states at the Fermi level with different possibilities of occupation of interslab T′ and intraslab T positions.

TABLE IV. Curie temperatures with different occupations of the interslab and intraslab sites by Si and Ge in the FM O(I) and FM M structures of $Tb_5Si_{2.2}Ge_{1.8}$.

	Curie temperature (K)	
Site occupation	O(I) FM	M FM
T′ Ge and T Ge positions	119	62
T′ Si and T Si positions	121	70
T′ Ge and T Si positions	99	64
T′ Si and T Ge positions	120	80

where $j_{i,i+\delta}$ is an exchange coupling constant between the spin $\vec{S}_i$ and its nearest neighbor spin $\vec{S}_{i+\delta}$, which are separated by δ. Then, the Curie temperature of a conventional three-dimensional Heisenberg ferromagnet in the mean field approximation is given by[66]

$$T_C = \frac{2}{3}\frac{E_{\mathrm{AFM}} - E_{\mathrm{FM}}}{k_B}.$$

Here, $E_{\mathrm{AFM}} - E_{\mathrm{FM}}$ is the energy required to align neighboring slabs ferromagnetically (i.e., the interslab exchange energy), and k_B is Boltzmann's constant. $E_{\mathrm{AFM}} - E_{\mathrm{FM}}$ is estimated by calculating the total energy difference between the AFM- and FM-aligned nearest neighbor slabs. The AFM structure is constructed in such a way that 10 Tb atoms/cell that belong to the same slab are aligned ferromagnetically, but the remaining 10 Tb atoms/cell that belong to the neighboring slab are aligned ferromagnetically in the opposite direction. In these calculations, the O(I) and M symmetries have been converted into the equivalent triclinic structures with P1 symmetry so that each of the 36 atoms in the unit cell is formally no longer equivalent to any other atom in the same unit cell.[38] This helps to assign any configuration of Tb spins.

The calculated Curie temperatures with different possible occupations of the interslab T′ and intraslab T sites are shown in Table IV. The Curie temperature increases when the interslab positions are occupied by Si atoms. The greatest increase is observed when switching from Ge in T′ and Si in T to Si in T′ and Ge in T. Considering the difference in size of Si and Ge atoms, bringing the neighboring slabs closer together promotes ferromagnetism, which also can be achieved by applying uniaxial pressure along the *b*-axis.

Finite temperature properties of a material can be calculated by coupling first principles outputs (e.g., magnetic moments and Curie temperatures [T_C]) to magnetothermodynamic models and solving them self consistently. To determine the magnetostructural transition temperature, we calculate the magnetization and magnetic entropy separately for each of the two phases and then compute the free energies. The temperature at which the free energies are equal for both structures represents a magnetostructural transition temperature. Figure 6 shows the change in magnetic free energy in both the O(I) and M phases of $Tb_5Si_{2.2}Ge_{1.8}$, calculated using the free energy relation[67]

$$F = -\frac{3}{2}\frac{J}{J+1}RT_C\sigma^2 - TS_M$$

where

$$S_M \approx R\left[\ln(2J+1) - \frac{3}{2}\left(\frac{J}{J+1}\right)\sigma^2 - \frac{9}{20}\frac{(2J+1)^4 - 1}{[2(J+1)]^4}\sigma^4\right], \text{ and}$$

$$\sigma = \frac{M}{M_S} = \tanh\left[\frac{3J}{J+1}\frac{M}{M_S}\frac{T_C}{T}\right].$$

Here, S_M and σ are magnetic entropy and renormalized magnetization. R is the universal gas constant, and J is the sum of spin and orbital angular momentum quantum numbers.

Each of the polymorphs, O(I) $Tb_5Si_{2.2}Ge_{1.8}$ and M $Tb_5Si_{2.2}Ge_{1.8}$, orders magnetically via a conventional second-order phase transition with the ${T_C}^{O(I)}$ of the O(I), $Tb_5Si_{2.2}Ge_{1.8}$ being considerably higher than the ${T_C}^{M}$ of the M polymorph (Table IV; Fig. 8, dotted curves). As shown in Fig. 6, when M $Tb_5Si_{2.2}Ge_{1.8}$ is cooled, its free energy initially remains lower than that of the O(I) $Tb_5Si_{2.2}Ge_{1.8}$. On further cooling, the free energies of the two polymorphs become equal at $T_M = 96$ K. Below T_M, the free energy of

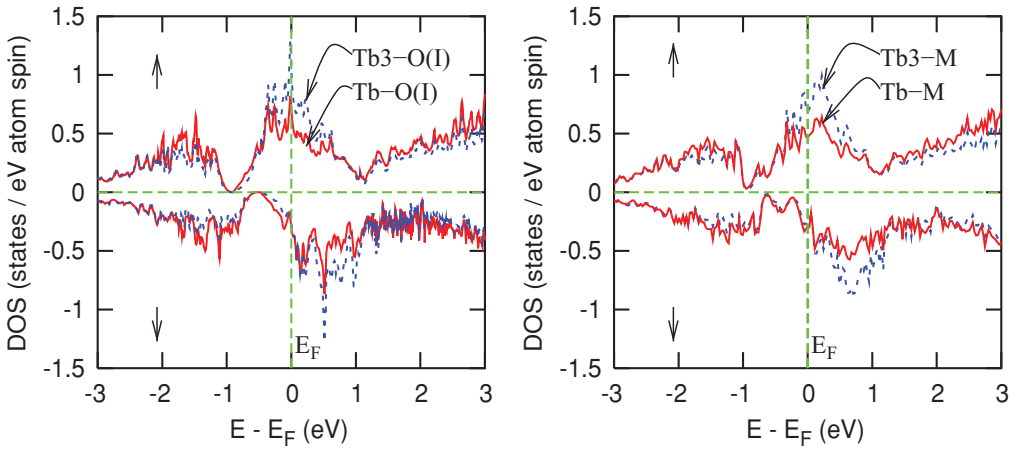

FIG. 4. (Color online) Comparison of 5*d* DOS averaged over all Tb atoms and 5*d* DOS of Tb3 atom in the O(I) (left) and M (right) structures of $Tb_5Si_{2.2}Ge_{1.8}$. Behavior of the average and individual 5*d* DOS are similar, but the average DOS is lower than the same of Tb3 at the Fermi level.

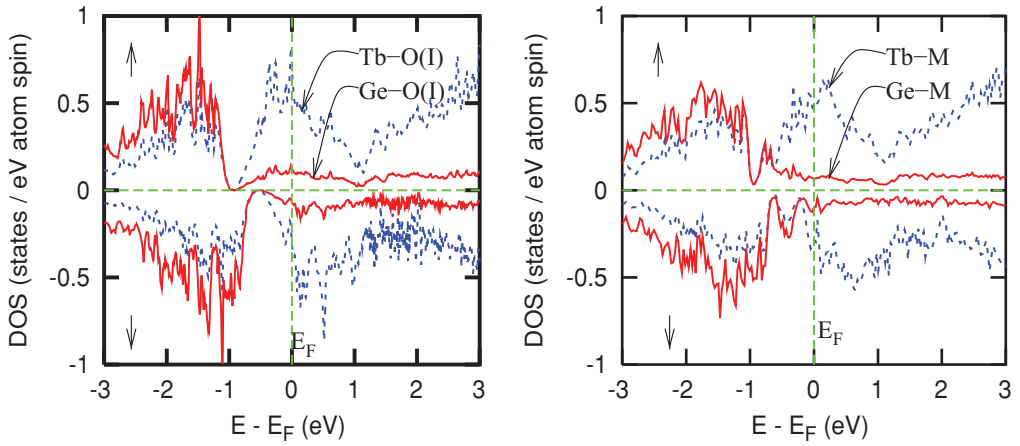

FIG. 5. (Color online) Comparison of average 5*d* DOS of Tb atoms and interslab 4*p* Ge atoms in the O(I) and M structures of $Tb_5Si_{2.2}Ge_{1.8}$.

the O(I) polymorph becomes lower than the M polymorph. This polymorphic transition at T_M also involves ferromagnetic ordering, with a large, discontinuous increase of the spontaneous magnetization (Fig. 8). Therefore, theory predicts that at $T_M = 96$ K, there is a magnetostructural transition. Furthermore, when a magnetic field is applied just above T_M, it changes the balance of the free energies between the PM M and FM O(I) phases, which in turn triggers a crystallographic transition between the two polymorphs that have different magnetizations, leading to a metamagnetic-like, discontinuous change of the magnetization at various temperature-specific critical fields.[29] It should be noted that the value of the magnetostructural transition temperature, $T_M = 96$ K, has been computed using the first mixing approach when, in one model, T and T′ sites were occupied by Si, and in another model, these were occupied by Ge. The second mixing approach results in the magnetostructural transition temperature of 92 K. Hence, both approaches predict nearly identical magnetostructural transition temperatures. Therefore, below, we will only show results of calculations using the first mixing approach.

The free energy analysis points to a simultaneous structural and magnetic transition, whereas experimentally, they are narrowly decoupled. To check whether this theoretical result can be improved, the electronic structure calculations have been repeated with the same O(I) unit cell volume for both the O(I) and M $Tb_5Si_{2.2}Ge_{1.8}$. This leads to a slight increase of the 5*d* moments of Tb atoms in M $Tb_5Si_{2.2}Ge_{1.8}$. Hence, the exchange coupling energy in the M $Tb_5Si_{2.2}Ge_{1.8}$ increases and the Curie temperature of the M $Tb_5Si_{2.2}Ge_{1.8}$ increases from 66 to 78 K. The magnetostructural transition temperature becomes 102 K, which is higher than the magnetostructural transition temperature obtained with the use of different unit cell volumes of O(I) and M structures. This shows that the magnetostructural transition temperature is always higher than the Curie temperature of the monoclinic polymorph and lower than that of the O(I) polymorph in $Tb_5Si_{2.2}Ge_{1.8}$.

Figure 7 shows the variation of the magnetic entropies with temperature in the O(I) and M structures assuming ferromagnetic ordering at their respective T_C. The magnetic entropy change, ΔS_M, at the magnetostructural transition temperature $T_M = 96$ K is -20 J/kg K. We note that as

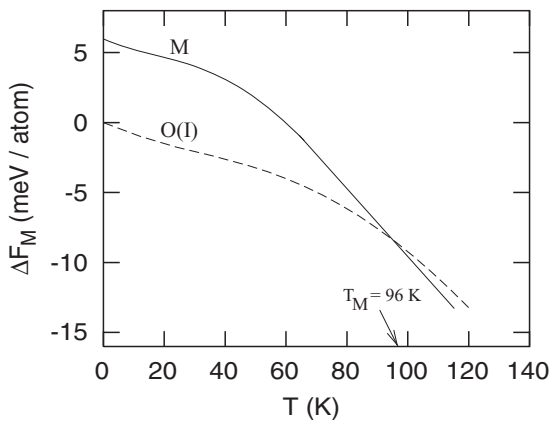

FIG. 6. Change in the magnetic free energy calculated using magnetic entropies and magnetization obtained from respective saturated magnetic moments and Curie temperature of the O(I) and M phases of $Tb_5Si_{2.2}Ge_{1.8}$.

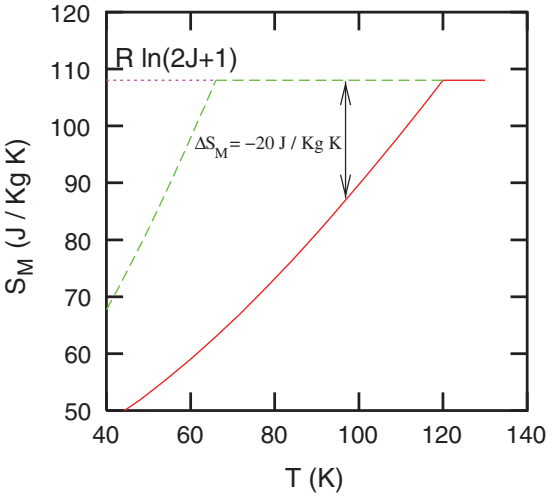

FIG. 7. (Color online) Magnetic entropy of the O(I) and M structures of $Tb_5Si_{2.2}Ge_{1.8}$ as a function of temperature. The magnetic entropy change at the magnetostructural transition temperature is -20 J/kg K. The magnitude of magnetic entropy change increases with the decrease of magnetostructural transition temperature.

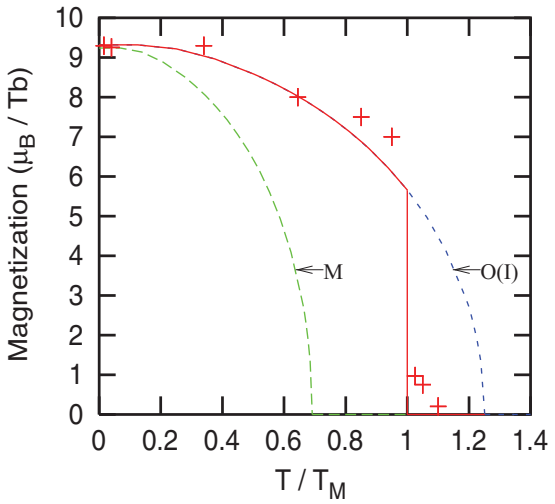

FIG. 8. (Color online) Magnetization as a function of temperature computed using the predicted magnetostructural transition temperature from the free energy analysis. At the magnetostructural transition temperature, T_M, the FM-ordered O(I) $Tb_5Si_{2.2}Ge_{1.8}$ transforms into M $Tb_5Si_{2.2}Ge_{1.8}$, which must be already PM at T_M, thus resulting in a discontinuous change of the magnetization. The solid line follows the magnetization of the system as temperature varies. The symbols represent the experimental values of magnetization of $Tb_5Si_{2.2}Ge_{1.8}$ in the *a*-axis.

the magnetostructural transition temperature decreases, the magnetic entropy change $(-\Delta S_M)$ becomes larger and larger, potentially reaching -40 to -45 J/kg K if T_C^M and $T_C^{O(I)}$ remain constant but T_M is reduced to $\sim$70 K.

The experimentally observed maximum entropy change for a single crystal with the magnetic field vector parallel to different crystallographic directions *a*, *c*, and *b* are -40 J/kg K, -38 J/kg K, and -3.6 J/kg K.[47] These differences are due to anisotropy on the magnetocaloric effect of $Tb_5Si_{2.2}Ge_{1.8}$. The theoretically calculated magnetic entropy change should be compared with the values observed along the easy magnetization direction, which is the *a*-axis. A part of the difference ($\sim$10 J/kg K[29]) between the calculated and experimentally measured entropy change along the easy magnetization direction reflects the contribution from the structural change, which is not accounted for in the magnetic entropy curves shown in Fig. 7 (also see our recent publications describing the difference in the $Gd_5Si_2Ge_2$ system).[15,29]

In Fig. 8, magnetization as a function of temperature renormalized to the magnetostructural transition temperature is computed and compared with the experimentally observed spontaneous magnetic moments extrapolated to zero magnetic field from the isothermal magnetization data corresponding to different temperatures.[27,47] As follows from Fig. 8, there is a good agreement between theoretically calculated and experimentally observed values of temperature-dependent magnetic moments of Tb atoms in $Tb_5Si_{2.2}Ge_{1.8}$. This shows that the theoretical approach presented here is capable of reproducing magnetic moments at finite temperature.

V. SUMMARY

The lower value of the total energy in the FM O(I) phase compared with the FM M phase confirms the stability of the FM O(I) $Tb_5Si_{2.2}Ge_{1.8}$ phase at low temperature. The calculated magnetic moments of Tb atoms in the FM O(I) $Tb_5Si_{2.2}Ge_{1.8}$ are larger than in the FM M $Tb_5Si_{2.2}Ge_{1.8}$. The magnetic exchange coupling energy of the orthorhombic phase is higher than that of the monoclinic phase, giving rise to a higher Curie temperature in the O(I) phase than in the M phase. The calculations show that the strain energy due to structural change is not immediately compensated by the magnetic exchange energy; hence, the system may remain in the ferromagnetic state over a small range of temperature, even after the structural change, which is observed experimentally. The magnetic moment as a function of temperature calculated using the Brillouin function with inputs from first principles agrees with the corresponding experimental values. The magnetostructural transition and magnetocaloric effect in $Tb_5Si_{2.2}Ge_{1.8}$ have been estimated by coupling the electronic structure with the magnetothermodynamic model. This approach closely reproduces the magnetostructural transition temperature observed experimentally. The magnetic entropy change at the magnetostructural transition temperature is smaller than the experimental value along the easy magnetization direction, which is related to the unaccounted difference in the lattice entropies of O(I) and M $Tb_5Si_{2.2}Ge_{1.8}$. The magnetic entropy change increases with a decrease of the magnetostructural transition temperature, which indicates a pathway toward tuning the magnitude of the magnetocaloric effect.

ACKNOWLEDGMENTS

The Ames Laboratory is operated by Iowa State University of Science and Technology for the US Department of Energy under Contract No. DE-AC02-07CH11358. This work was supported by the Office of Basic Energy Sciences, Materials Science and Engineering Division of the Office of Science.

*durga@ameslab.gov

[1] A. M. Tishin and Y. I. Spichkin, *The Magnetocaloric Effect and its Applications* (Institute of Physics, Bristol and Philadelphia, 2003).
[2] K. A. Gschneidner Jr., V. K. Pecharsky, and A. O. Tsokol, Rep. Prog. Phys. **68**, 1479 (2005), and references therein.
[3] V. K. Pecharsky and K. A. Gschneidner Jr., J. Magn. Magn. Mater. **200**, 44 (1999).
[4] E. Bruck, J. Phys. D **38**, R381 (2005).
[5] V. K. Pecharsky and K. A. Gschneidner Jr., Adv. Mater. (Weinheim) **13**, 683 (2001).
[6] F. X. Hu, B. G. Shen, J. R. Sun, Z. H. Cheng, G. H. Rao, and X. X. Zhang, Appl. Phys. Lett. **78**, 3675 (2001).
[7] H. Wada and Y. Tanabe, Appl. Phys. Lett. **79**, 3302 (2001).

[8] W. Chen, W. Zhong, C. F. Pan, H. Chang, and Y. W. Du, Acta Phys. Sin. **50**, 319 (2001).

[9] V. K. Pecharsky and K. A. Gschneidner Jr., Pure Appl. Chem. **79**, 1383 (2007).

[10] V. K. Pecharsky, A. P. Holm, K. A. Gschneidner Jr., and R. Rink, Phys. Rev. Lett. **91**, 197204 (2003).

[11] Ya. Mudryk, A. P. Holm, K. A. Gschneidner Jr., and V. K. Pecharsky, Phys. Rev. B **72**, 064442 (2005).

[12] L. Morellon, P. A. Algarabel, M. R. Ibarra, J. Blasco, and B. García-Landa, Phys. Rev. B **58**, R14721 (1998).

[13] L. Morellon, J. Blasco, P. A. Alrarabel, and M. R. Ibarra, Phys. Rev. B **62**, 1022 (2000).

[14] W. Choe, V. K. Pecharsky, A. O. Pecharsky, K. A. Gschneidner Jr., V. G. Young Jr., and G. J. Miler, Phys. Rev. Lett. **84**, 4617 (2000).

[15] V. K. Pecharsky and K. A. Gschneidner Jr., in *Magnetism and Structure in Functional Materials*, edited by A. Planes, L. Manosa, and A. Saxena, Vol. 79 Springer Series in Materials Science (Springer, Heidelberg, 2005).

[16] Ya. Mudryk, Y. Lee, T. Vogt, K. A. Gschneidner Jr., and V. K. Pecharsky, Phys. Rev. B **71**, 174104 (2005).

[17] C. Magen, L. Morellon, P. A. Algarabel, M. R. Ibarra, Z. Arnold, J. Kamarad, T. A. Lograsso, D. L. Schlagel, V. K. Pecharsky, A. O. Tsokol, and K. A. Gschneidner Jr., Phys. Rev. B **72**, 024416 (2005).

[18] E. M. Levin, V. K. Pecharsky, and K. A. Gschneidner Jr., Phys. Rev. B **62**, R14625 (2000).

[19] H. Tang, A. O. Pecharsky, D. L. Schlagel, T. A. Lograsso, V. K. Pecharsky, and K. A. Gschneidner Jr., J. Appl. Phys. **93**, 8298 (2003).

[20] V. K. Pecharsky and K. A. Gschneidner Jr., Phys. Rev. Lett. **78**, 4494 (1997).

[21] L. Morellon, C. Magen, P. A. Algarabel, M. R. Ibarra, and C. Ritter, Appl. Phys. Lett. **79**, 1318 (2001).

[22] C. Ritter, L. Morellon, P. A. Algarabel, C. Magen, and M. R. Ibarra, Phys. Rev. B **65**, 094405 (2002).

[23] L. Morellon, C. Ritter, C. Magen, P. A. Algarabel, and M. R. Ibarra, Phys. Rev. B **68**, 024417 (2003).

[24] V. K. Pecharsky and K. A. Gschneidner Jr., Appl. Phys. Lett. **70**, 3299 (1997).

[25] A. O. Pecharsky, K. A. Gschneidner Jr., V. K. Pecharsky, and C. E. Schindler, J. Alloys Compd. **338**, 126 (2002).

[26] L. Morellon, Z. Arnold, C. Magen, C. Ritter, O. Prokhnenko, Y. Skorokhod, P. A. Algarabel, M. R. Ibarra, and J. Kamarad, Phys. Rev. Lett. **93**, 137201 (2004).

[27] V. O. Garlea, J. L. Zarestky, C. Y. Jones, L.-L. Lin, D. L. Schlagel, T. A. Lograsso, A. O. Tsokol, V. K. Pecharsky, K. A. Gschneidner Jr., and C. Stassis, Phys. Rev. B **72**, 104431 (2005).

[28] M. Zou, V. K. Pecharsky, K. A. Gschneidner Jr., D. L. Schlagel, and T. A. Lograsso, Phys. Rev. B **78**, 014435 (2008).

[29] D. Paudyal, V. K. Pecharsky, K. A. Gschneidner Jr., and B. N. Harmon, Phys. Rev. B **73**, 144406 (2006).

[30] V. K. Pecharsky, G. D. Samolyuk, V. P. Antropov, A. O. Pecharsky, and K. A. Gschneidner Jr., J. Solid State Chem. **171**, 57 (2003).

[31] G. D. Samolyuk and V. P. Antropov, J. Appl. Phys. **91**, 8540 (2002).

[32] G. D. Samolyuk and V. P. Antropov, J. Appl. Phys. **97**, 10A310 (2005).

[33] B. N. Harmon and V. N. Antonov, J. Appl. Phys. **91**, 9815 (2002).

[34] B. N. Harmon and V. N. Antonov, J. Appl. Phys. **93**, 4678 (2003).

[35] H. Tang, V. K. Pecharsky, G. D. Samolyuk, M. Zou, K. A. Gschneidner Jr., V. P. Antropov, D. L. Schlagel, and T. A. Lograsso, Phys. Rev. Lett. **93**, 237203 (2004).

[36] G. Skorek, J. Deniszczyk, and J. Szade, J. Phys. Condens. Matter **14**, 7273 (2002).

[37] D. Paudyal, V. K. Pecharsky, K. A. Gschneidner Jr., and B. N. Harmon, Phys. Rev. B **75**, 094427 (2007).

[38] D. Paudyal, V. K. Pecharsky, and K. A. Gschneidner Jr., J. Phys. Condens. Matter **20**, 235235 (2008).

[39] D. Paudyal, Ya. Mudryk, V. K. Pecharsky, and K. A. Gschneidner Jr., Phys. Rev. B **82**, 144413 (2010).

[40] Y. Mudryk, D. Paudyal, V. K. Pecharsky, K. A. Gschneidner Jr., S. Misra, and G. J. Miller, Phys. Rev. Lett. **105**, 066401 (2010).

[41] D. Paudyal, Ya. Mudryk, V. K. Pecharsky, S. Misra, G. J. Miller, and K. A. Gschneidner Jr., J. Appl. Phys. **107**, 09A908 (2010).

[42] Ya. Mudryk, D. Paudyal, V. K. Pecharsky, and K. A. Gschneidner Jr., Phys. Rev. B **77**, 024408 (2008).

[43] A. S. Chernyshov, Ya. Mudryk, D. Paudyal, V. K. Pecharsky, K. A. Gschneidner Jr., D. L. Schlagel, and T. A. Lograsso, Phys. Rev. B **80**, 184416 (2009).

[44] N. K. Singh, D. Paudyal, Ya. Mudryk, V. K. Pecharsky, and K. A. Gschneidner Jr., Phys. Rev. B **79**, 094115 (2009).

[45] N. K. Singh, D. Paudyal, Ya. Mudryk, V. K. Pecharsky, and K. A. Gschneidner Jr., Phys. Rev. B **81**, 184414 (2010).

[46] N. K. Singh, D. Paudyal, V. K. Pecharsky, and K. A. Gschneidner Jr., J. Appl. Phys. **107**, 09A921 (2010).

[47] M. Zou, Ya. Mudryk, V. K. Pecharsky, K. A. Gschneidner Jr., D. L. Schlagel, and T. A. Lograsso, Phys. Rev. B **75**, 024418 (2007).

[48] V. K. Pecharsky and K. A. Gschneidner Jr., J. Alloys Compd. **260**, 98 (1997).

[49] V. I. Anisimov, F. Aryasetiawan, and A. I. Lichtenstein, J. Phys. Condens. Matter. **9**, 767 (1997).

[50] B. N. Harmon, V. P. Antropov, A. I. Lichtenstein, I. V. Solovyeb, and V. I. Anisimov, J. Phys. Chem. Solids **56**, 1521 (1995).

[51] O. K. Andersen and O. Jepsen, Phys. Rev. Lett. **53**, 2571 (1984).

[52] S. Lebègue, A. Svane, M. I. Katsnelson, A. I. Lichtenstein, and O. Eriksson, J. Phys. Condens. Matter **18**, 6329 (2006).

[53] U. von Barth and L. Hedin, J. Phys. C **5**, 1629 (1972).

[54] R. M. White, *Quantum Theory of Magnetism*, 3rd ed. (Springer-Verlag, Berlin, Heidelberg, 2007), Chap. 9, p. 286.

[55] M. S. S. Brooks and B. Johansson, in *Hand Book of Magnetic Materials*, edited by K. H. J. Buschow (Elsevier Science, North-Holland, 1993), Vol. 7, Chap. 3, p. 139.

[56] J. Jensen and A. R. Mackintosh, *Rare Earth Magnetism Structures and Excitations* (Clarendon Press, Oxford, 1991), Chap. 1, p. 45.

[57] M. Richter, J. Phys. D: Appl. Phys. **31**, 1017 (1998).

[58] R. Ahuja, S. Auluck, B. Johansson, and M. S. S. Brooks, Phys. Rev. B **50**, 5147 (1994).

[59] F. Gerken and Schmidt-May, J. Phys. F: Met. Phys. **13**, 1571 (1983).

[60] K. W. H. Stevens, Proc. Phys. Soc. A **65**, 209 (1952).
[61] Y. C. Tseng, H. J. Ma, C. Y. Yang, Y. Mudryk, V. K. Pecharsky, K. A. Gschneidner Jr., N. M. Souza-Neto, and D. Haskel, Phys. Rev. B **83**, 104419 (2011).
[62] A. P. Holm, V. K. Pecharsky, and K. A. Gschneidner Jr. (unpublished).
[63] R. Nirmala, Ya Mudryk, V. K. Pecharsky, and K. A. Gschneidner Jr., Phys. Rev. B **76**, 104417 (2007).
[64] V. K. Pecharsky, A. O. Pecharsky, Y. Mozharivskyj, K. A. Gschneidner Jr., and G. J. Miller, Phys. Rev. Lett. **91**, 207205 (2003).
[65] A. B. Shick, W. E. Pickett, and C. S. Fadley, Phys. Rev. B **61**, R9213 (2000).
[66] Ph. Kurz, G. Bihlmayer, and S Blügel, J. Phys. Condens. Matter **14**, 6353 (2002).
[67] C. P. Bean and D. S. Rodbell, Phys. Rev. **126**, 104 (1962).